Particle size dependent exchange bias and cluster-glass states in $LaMn_{0.7}Fe_{0.3}O_3$

2008 J. Phys.: Condens. Matter 20 195215

(http://iopscience.iop.org/0953-8984/20/19/195215)

J. Phys.: Condens. Matter **20** (2008) 195215 (5pp) doi:10.1088/0953-8984/20/19/195215

Particle size dependent exchange bias and cluster-glass states in $LaMn_{0.7}Fe_{0.3}O_3$

M Thakur, M Patra, K De, S Majumdar and S Giri

Department of Solid State Physics and Center for Advanced Materials, Indian Association for the Cultivation of Science, Jadavpur, Kolkata 700 032, India

E-mail: sspsg2@iacs.res.in (S Giri)

Received 2 January 2008, in final form 26 February 2008
Published 11 April 2008
Online at stacks.iop.org/JPhysCM/20/195215

Abstract

The cluster-glass compound $LaMn_{0.7}Fe_{0.3}O_3$ was synthesized with average particle sizes ∼20, ∼90, and ∼300 nm. We observed a shift of the magnetic hysteresis loop in the field axis while the sample was cooled in an external magnetic field. The systematic shift of the hysteresis loops and the cooling field dependence of the shift indicated the phenomenon of exchange bias. The exchange bias field was found to be strongly dependent on the particle size, where the exchange bias field decreased considerably with an increase of particle size, and the weak effect of exchange bias was observed for particles with size ∼300 nm. A cluster-glass state with short range ferromagnetic clusters embedded in the spin-glass like host has been proposed, where the average size of the ferromagnetic cluster increases with particle size.

(Some figures in this article are in colour only in the electronic version)

1. Introduction

Exchange bias is a phenomenon associated with induced exchange anisotropy at the interface between ferromagnetic (FM) and antiferromagnetic (AFM) phases in a heterogeneous system [1–3]. The exchange bias considerably increases the total anisotropy of the system, which has technological applications for magnetic storage, spin-electron devices, and the development of permanent magnets. The exchange bias is observed by the unidirectional shift of the hysteresis loop when the system is cooled down to low temperatures in an external magnetic field through the Néel temperature. In addition to the exchange bias at the FM/AFM interface, exchange bias has also been reported for different systems involved with glassy magnetic behaviour such as FM/spin-glass (SG) bilayer films, FM nanoparticles in a glassy matrix or FM/glassy magnetic core–shell structure, and intrinsically phase separated cluster-glass (CG) compounds [4–9].

In most cases, the exchange bias has been investigated on artificially fabricated heterogeneous systems consisting of FM/AFM or FM/SG bilayers or core–shell structures. The observation of exchange bias in the intrinsically phase separated compound is fascinating not only for technological applications, but also for a fundamental understanding of the nature of intrinsic phase separation of the compounds. To the best of our knowledge, very few systems have been reported so far, where exchange bias is ascribed to intrinsic phase separation between FM/AFM or FM/SG states. In the case of charge ordered manganites such as $Pr_{1/3}Ca_{2/3}MnO_3$ and $Y_{0.2}Ca_{0.8}MnO_3$, the strong effect of exchange bias is reported at the FM/AFM interface, where exchange bias is ascribed to the intrinsic phase separation [10, 11]. The exchange bias is also reported for cluster-glass cobaltites $La(Ba, Sr)CoO_3$, where exchange bias is suggested due to the cluster-glass state consisting of FM and SG phases [8, 9]. Recently we observed the exchange bias phenomenon in $LaMnO_3$ as a result of Fe substitution, where exchange bias was also attributed to the cluster-glass state in $LaMn_{0.7}Fe_{0.3}O_3$ [12]. The scenario of FM clusters embedded in the SG-like host has also been proposed for $La_{1-\delta}Mn_{0.7}Fe_{0.3}O_3$ with $\delta = 0$ and 0.13 based on dc magnetization, ac susceptibility, and electron spin resonance (ESR) studies [13, 14]. In fact, the coexistence of FM and glassy magnetic interactions was suggested in our earlier report for both the La-stoichiometric and La-deficient lanthanum manganite as a result of Fe substitution [15–17].

In this report, we investigate the particle size dependent exchange bias phenomenon and the nature of cluster-glass states in $LaMn_{0.7}Fe_{0.3}O_3$. Until now the particle size dependence exchange bias phenomenon have not been reported in intrinsically phase separated compounds. Here, we found that the exchange bias is strongly dependent on the average size of the particles. The exchange bias field decreases significantly

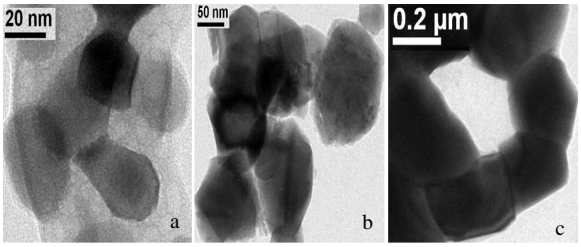

Figure 1. TEM image of S20 (a), S90 (b), and S300 (c).

with the increase of particle size, where the weak effect of exchange bias is noticed for the particles with size ∼300 nm. The particle size dependent intrinsic phase separation scenario has been suggested to explain the significant effect of exchange bias on particle size.

2. Experiment

The polycrystalline sample $LaMn_{0.7}Fe_{0.3}O_3$ was prepared by the chemical route, which was described in our previous report [15]. The as-synthesized sample was heated at 600, 800, and 1200 °C, where the average size of the particles are found to be ∼20 ± 5, ∼90 ± 10, and ∼300 ± 20 nm, respectively. The sizes of the particles are observed by transmission electron microscopy (TEM) images, using model ZEOL JEM-2010, as seen in figure 1. Note that citric acid was used in the chemical synthesis, where the existence of citrate precursor is shown in figure 1(a) by the light shaded background. The citrate precursor was decomposed when the sample was heated at higher temperatures. The single phase of the crystal structure was confirmed by a powder x-ray diffractometer (Seifert XRD 3000P) using Cu Kα radiation. The powder x-ray diffraction patterns are characterized by a single phase of orthorhombic (*Pnma*) structure for S20, S90, and S300, which is consistent with our earlier report [13–17]. Henceforth, we address S20, S90, and S300 for the particles with average diameters 20, 90, and 300 nm, respectively. The dc magnetization and ac susceptibility were measured using a commercial superconducting quantum interference device (SQUID) magnetometer (MPMS, XL). In the case of zero-field cooled (ZFC) conditions, the sample was cooled down to the desired temperature in zero field, while for field-cooled (FC) conditions the sample was cooled in an external magnetic field.

3. Experimental results and discussions

Temperature variation of magnetization measured at 100 Oe are shown in figures 2(a)–(c) for S20, S90, and S300, respectively when the sample was cooled under ZFC conditions. The high temperature peak (T_p) and a shoulder at low temperature (T_f) are observed for all cases, consistent with reported results for bulk $LaMn_{0.7}Fe_{0.3}O_3$. We measure the ac susceptibility at 100 Hz and H_{ac} = 3.0 Oe for S300. The signature of T_f is clearly observed by a broad maximum in the imaginary part of the ac susceptibility (χ_{ac}), while the real part exhibits a similar temperature dependence to the

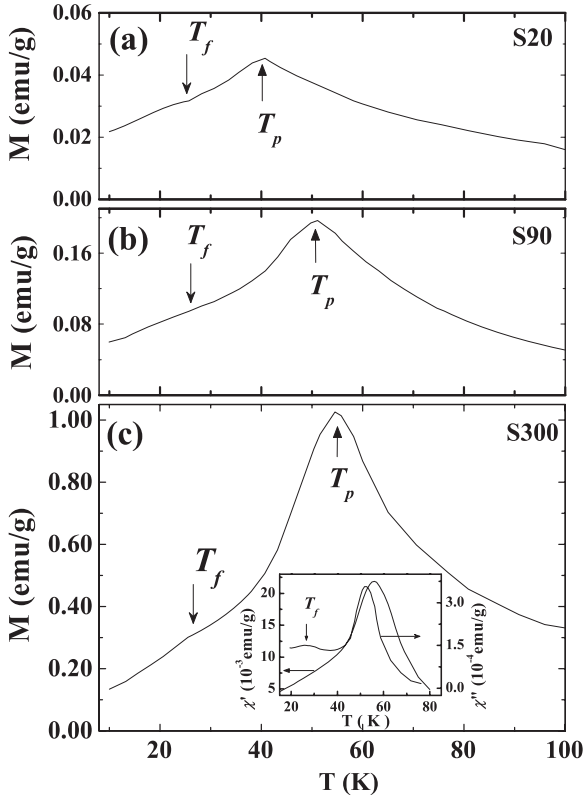

Figure 2. Temperature dependence of magnetization for S20 (a), S90 (b), and S300 (c). The arrows indicate the position of T_f and T_p. The inset of (c) exhibits the temperature dependence of the real and imaginary part of the ac susceptibility.

dc magnetization, as seen in the inset of figure 2(c). The details of the frequency dependence of T_f for S300 have been characterized in our earlier report, exhibiting an SG-like transition at T_f [13]. Here, the ac susceptibility was also measured for S90 and S20, where the magnitude of χ_{ac} was so small that we could not detect it within our instrumental resolution. However, we additionally observed that T_p increases consistently from 40 to 55 K with the increase of average particle size as seen in figure 2. The magnitude of the ZFC magnetization increases considerably with the size of the particles. We measure the magnetic hysteresis for S20, S90, and S300 after zero-field cooling at 5 K (figure 3), where the magnetization curves do not show any saturating tendency even at 50.0 kOe. In addition, the magnetization at 50.0 kOe and the remanence of magnetization increases considerably, while a small decrease of coercivity (H_C) is observed with an increase of particle size, as seen in the inset of figure 3. In order to understand the origin of T_p and variation of T_p with particle size, the magnetic hysteresis was measured at different temperatures for S90, where typical examples of temperature dependence of magnetic hysteresis at selective temperatures are shown in figure 4. The coercivity vanishes around T_p, as seen in the inset of the top panel of figure 4. In the bottom panel of figure 4, the plots of magnetization against H/T at 60 and 80 K (above T_p) are shown, which almost overlap each other and could be fitted satisfactorily with a single Langevin function as seen by the continuous curves in the figure. The

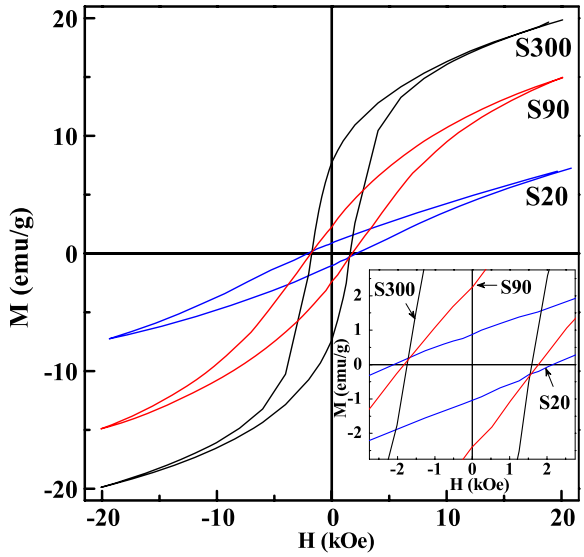

Figure 3. Magnetic hysteresis loops after zero-field cooling at 5 K for S20, S90, and S300.

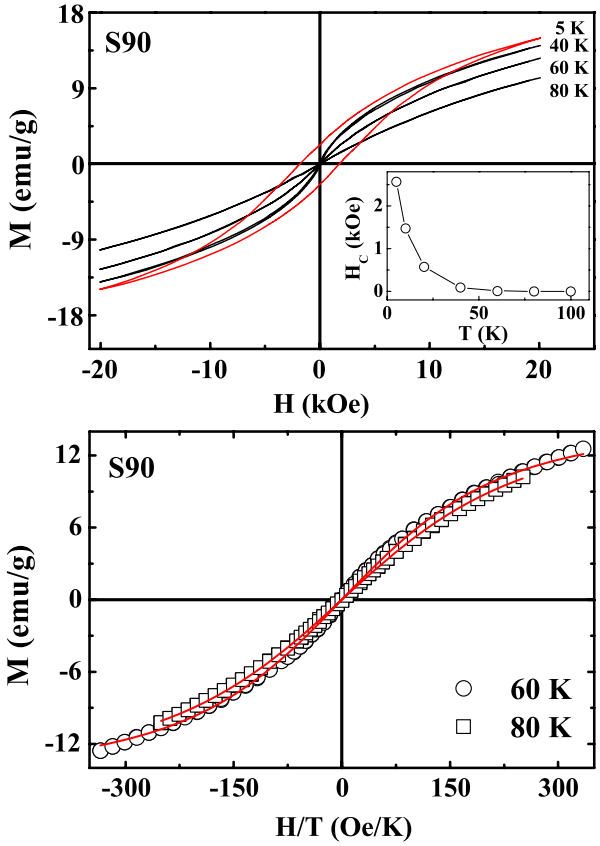

Figure 4. Top panel: magnetic hysteresis loops at selective temperatures for S90. The inset shows the plot of coercivity (H_C) as a function of temperature. Bottom panel: the plots of magnetization against H/T at 60 and 80 K, which almost overlap each other. The continuous curves show the fits of the experimental data using the Langevin function.

features of the magnetization curves above T_p are consistent with the typical superparamagnetic behaviour. Note that the magnetization curves are fitted by a single Langevin function, which indicates the narrow size distribution of the size of FM clusters. The average size of the FM cluster is estimated to be ∼5.0 nm from the fit of the magnetization curve using the Langevin function. In the case of non-interacting or weakly interacting FM nanoparticles embedded in a non-magnetic matrix, the blocking temperature increases with the particle size, where the magnitudes of the ZFC magnetization and saturation magnetization are found to increase with particle size [7, 18]. In the present observation, the magnetization results indicate that T_p behaves like a blocking temperature associated with the weakly interacting FM clusters, which are embedded in the glassy magnetic matrix. The increase of T_p indicates the increase of the average size of FM clusters. The coexistence of FM clusters and spin-glass like phases has been characterized by dc magnetization and ac susceptibility measurements, where the direct evidence of FM clusters was reported by Liu *et al* based on ESR studies [13, 14]. The above scenario is consistent with the CG state of the mixed-valent perovskites [8, 9, 19, 20]. Note that T_p might also be associated with the particle size effect instead of the effect of the FM cluster. However, it is difficult to explain the blocking temperature around ∼55 K for particles with average diameter around ∼300 nm. In fact, the estimate of the size of the FM cluster (∼5.0 nm) above T_p further confirms that T_p in the CG compound behaves like a superparamagnetic blocking temperature.

A shift of the magnetic hysteresis loop in the field axis is observed at 5 K for S20 while the sample was cooled down to 5 K from 250 K ($\gg T_f$) in ±6.0 kOe and the hysteresis loop was measured in between ±20.0 kOe. Shifts in the negative and positive directions of the field axis are observed when the sample was cooled in 6.0 and −6.0 kOe, respectively, as seen in figure 5. The shift is absent while cooling under ZFC conditions. The above features indicate the phenomenon of exchange bias. The value of the exchange bias field (H_E) is estimated from the shift of the centroid of the loop in the field axis, as described in figure 5. The values of H_E and the coercive field (H_C) are ∼800 Oe and 2.1 kOe, respectively, where the ratio of H_E and H_C is comparable to the reported results for other CG compounds with perovskite structure [8, 9, 21]. We observe that H_E is strongly influenced by the maximum value of magnetic field applied for the measurement of hysteresis. The magnitude of H_E is decreased to ∼150 Oe while the hysteresis loop was measured in between ±50.0 kOe.

The phenomenon of exchange bias was also investigated for S90 and S300. Interestingly, the exchange bias is considerable for S90 and weak for S300, while measurement was performed under identical conditions to those for S20. A small negative shift of the hysteresis is observed for S300 with $H_E \approx 30$ Oe, as seen in the inset of figure 5. Therefore, the magnetic hysteresis was measured only for S20 and S90 at different cooling field (H_{cool}) while loops were measured in between ±50 kOe. The H_{cool} dependence of H_E is shown in figure 6 for S20 and S90, where the value of H_E increases with H_{cool} and then decreases with further increase of H_{cool} for both cases. A similar H_{cool} dependence of H_E has also

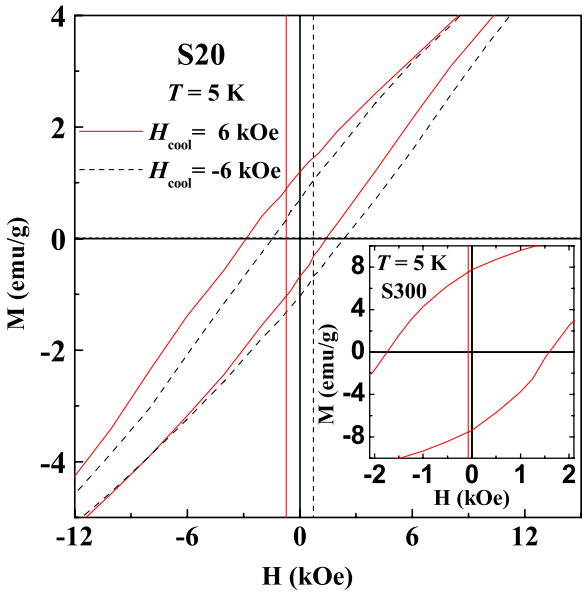

Figure 5. The central part of the magnetic hysteresis loops at 5 K is highlighted for S20, while the sample was cooled in 6 kOe (solid curve) and −6 kOe (dashed curve) for S20. The inset also exhibits the central part of the hysteresis loop at 5 K for S300, indicating a small exchange bias field.

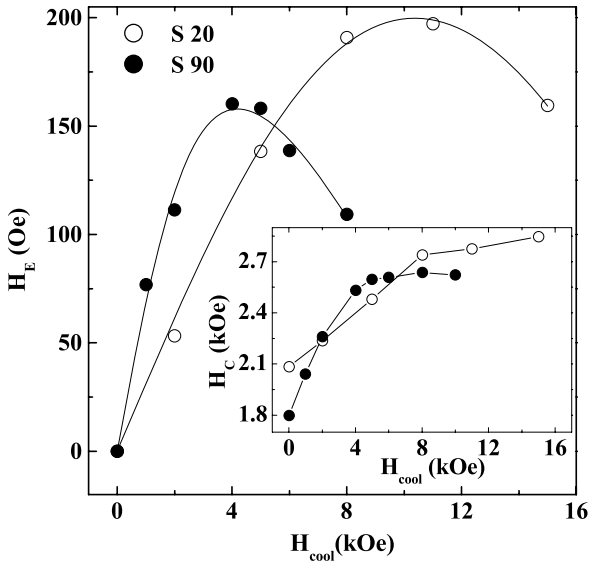

Figure 6. Cooling field ($H_{\rm cool}$) dependence of exchange bias field ($H_{\rm E}$) for S20 and S90. The solid lines show the fits as described in the text. The inset of the figure exhibits the coercivity ($H_{\rm C}$) against $H_{\rm cool}$ for S20 and S90. The solid lines are guides for the eye.

been reported for another CG compound $La_{1-x}Sr_xCoO_3$ and Fe nanoparticles in an iron oxide matrix, where the following explanation has been proposed [9, 22]. The glassy magnetic phase induces the *frozen* FM spins at the FM/SG interface, which leads to the exchange bias. In the case of low cooling field, $H_{\rm cool}$ is not strong enough to magnetize the *frozen* FM spins toward saturation. Therefore, the degree of alignment of the moment of the *frozen* FM spins is enhanced along a preferential direction with the increase of the $H_{\rm cool}$, which reduces the effect of averaging of the anisotropy due to randomness. The increase of anisotropy is indicated by the sharp increase of $H_{\rm C}$ with $H_{\rm cool}$ and the increasing trend of $H_{\rm C}$ becomes slower around ∼4.0 and ∼8.0 kOe, as seen in the inset of figure 6, where the broad peak in the $H_{\rm E}$ against $H_{\rm cool}$ graph is observed. When the cooling field is high enough, the *frozen* FM spins tend toward saturation and vary a little along the field with the further increase of $H_{\rm cool}$. In addition, the magnetic coupling between the strong cooling field and the glassy magnetic moments increases, tending to orient them along the field direction, where magnetic coupling dominates over exchange coupling, resulting in the decrease of $H_{\rm E}$ with the further increase of $H_{\rm cool}$. Note that the peak of the plot in figure 6 is observed around ∼4.2 and ∼10.5 kOe for S90 and S20, respectively. The above results are in accordance with the magnetic hysteresis at 5 K (figure 3), where the signature of larger anisotropy energy is indicated by the larger coercivity for S20 than S90. In the case of large anisotropy, a large magnetic field is required to saturate the magnetization, which is also indicated by the peak in the $H_{\rm E}$ against $H_{\rm cool}$ plot at higher cooling field for S20 than S90. In addition, the value of $H_{\rm E}$ around the peak is significantly larger for S20 than for S90 and becomes weak for S300.

Recently, Niebieskikwiat and Salamon proposed a simplified exchange interaction model for $Pr_{1/3}Ca_{2/3}MnO_3$ to explain the $H_{\rm cool}$ dependence of $H_{\rm E}$, where small and weakly interacting FM clusters are assumed to be embedded in an SG-like or AFM host material [10]. Despite the values of exchange bias field not being as large as observed in charge ordered compounds $Pr_{1/3}Ca_{2/3}MnO_3$, a trial was made to fit the $H_{\rm cool}$ dependence of $H_{\rm E}$ with the model using the following expression from [10], $H_{\rm E} \propto J_{\rm i}[\frac{J_{\rm i}\mu_0}{(g\mu_{\rm B})^2}L(\frac{\mu H_{\rm cool}}{k_{\rm B}T_f}) + H_{\rm cool}]$, where $J_{\rm i}$ is the interface exchange constant. We assume the magnetic moment of the FM cluster, $\mu = N_v\mu_0$, with $\mu_0 \approx 3\ \mu_{\rm B}$ for the FM Mn core spin, where N_v is the number of spins per FM cluster. The first term in the expression dominates for small $H_{\rm cool}$ ($\propto J_{\rm i}^2$), while for large $H_{\rm cool}$ the second term ($\propto J_{\rm i}$) dominates. The solid line in figure 6 exhibits a satisfactory fit of the experimental data using the above expression with $J_{\rm i}$ and μ as adjustable parameters. The values of $J_{\rm i}$ are ≈ -0.23 and -0.11 meV with $\mu \approx 51\mu_{\rm B}$ and $219\ \mu_{\rm B}$ for S20 and S90, respectively. Using the values of μ, N_v are ≈17 and 73 while the number density of FM clusters (n) can be estimated from the saturation magnetization to be $M_{\rm S} = n\mu$, which gives $n \approx 3.30 \times 10^{-6}$ and 7.23×10^{-5} Å^{-3} for S20 and S90, respectively. The value of n further gives us the rough estimate of the size of FM cluster ∼1.0 and 3.0 nm for S20 and S90, respectively. Here, the rough estimates of the average size of the FM clusters indicate that the size of the FM clusters increases with the particle size. Note that the size is reasonable with the size of the FM cluster (∼5.0 nm) obtained from the magnetization curve for S90. The exchange bias effect is typically developed when the sample was cooled in FC conditions. In the case of FC conditions a layer of *frozen* FM spins is developed on the outer surface of the FM clusters, where the frozen layer is created by the conversion of the surface part of the FM spins to the *frozen* FM spins, resulting

in a decrease of the effective size of the FM cluster compared with that of the actual size of the FM cluster. Consistent with the CG perovskite La(Ba, Sr)CoO_3, the experimental results in the present observation may also provide an indication of the exchange bias at the FM/SG-like interface in $LaMn_{0.7}Fe_{0.3}O_3$. Note that the effective interface area is one of the crucial factors for the exchange bias phenomenon. Here, the increase of the size of the FM clusters is indicated by several pieces of experimental evidence such as the H_{cool} dependence of H_E, and the increase of T_P and saturating magnetization with the increase of particle size. The increase of the size of the FM cluster decreases the effective interface area, which weakens the exchange coupling at the FM/SG-like interface and, thus, the exchange bias is weakened with the increase of particle size and becomes small for S300. The explanation is consistent with the model proposed by Meiklejohn, which predicts the relation to be $H_E \approx J_{ex}/M_{FM} \times t_{FM}$, where J_{ex} is the exchange constant across the FM/AFM interface per unit area, and M_{FM} and t_{FM} are the magnetization and the thickness of the FM layer, respectively [23]. In the present observation, the average size of the FM cluster analogous to t_{FM} and M_{FM} increases with the increase of particle size, which results in a decrease of the exchange bias field.

In conclusion, the cluster-glass compound $LaMn_{0.7}Fe_{0.3}O_3$ consists of short range FM clusters and SG-like phase, where the increase of the size of the FM clusters is observed by the increase of the particle size. Interestingly, we observe that the exchange bias is strongly dependent on the particle size, where exchange bias is weak for the sample with larger particles. We propose that the exchange bias in the cluster-glass compound is induced at the FM/SG-like interface, where the total area of the interface is decreased by the increase of particle size, resulting in a weakening of the exchange bias.

Acknowledgments

One of the authors (SG) wishes to thank CSIR (Project No. 03(999)04/EMR-II) and DST (Project No. SR/S2/CMP-46/2003), India for the financial support.

References

[1] Meiklejohn W H and Bean C P 1956 *Phys. Rev.* **102** 1413
[2] Nogues J, Sort J, Langlais V, Skumryev V, Surinach S, Munoz J S and Baro M D 2005 *Phys. Rep.* **422** 65
Nogues J, Sort J, Langlais V, Skumryev V, Surinach S, Munoz J S and Baro M D 2005 *Int. J. Nanotechnol.* **2** 23
Nogues J and Schuller I K 1999 *J. Magn. Magn. Mater.* **192** 203
[3] Stamps R L 2000 *J. Phys. D: Appl. Phys.* **33** R247
[4] Ali M, Adie P, Marrows C H, Greig D, Hickey B J and Stamp R L 2007 *Nat. Mater.* **6** 70
[5] Fiorani D, Del Bianco L, Testa A M and Trohidou K N 2007 *J. Phys.: Condens. Matter* **19** 225007
[6] Gruyters M 2005 *Phys. Rev. Lett.* **95** 077204
[7] Martnez-Boubeta C, Simeonidis K, Angelakeris M, Pazos-Prez N, Giersig M, Delimitis A, Nalbandian L, Alexandrakis V and Niarchos D 2006 *Phys. Rev.* B **74** 054430
[8] Luo W and Wang F 2007 *Appl. Phys. Lett.* **90** 162515
[9] Tang Y K, Sun Y and Cheng Z H 2006 *Phys. Rev.* B **73** 174419
Tang Y K, Sun Y and Cheng Z H 2006 *J. Appl. Phys.* **100** 023914
[10] Niebieskikwiat D and Salamon M B 2005 *Phys. Rev.* B **72** 174422
[11] Qian T, Li G, Zhang T, Zhou T F, Xiang X Q, Kang X W and Lia X G 2007 *Appl. Phys. Lett.* **90** 012503
[12] Patra M, De K, Majumdar S and Giri S 2007 *Eur. Phys. J.* B **58** 367
[13] De K, Patra M, Majumdar S and Giri S 2007 *J. Phys. D: Appl. Phys.* **40** 7614
[14] Liu X J, Li Z Q, Yu A, Liu M L, Li W R, Li B L, Wu P, Bai H L and Jiang E Y 2007 *J. Magn. Magn. Mater.* **313** 354
[15] De K, Ray R, Panda R N, Giri S, Nakamura H and Kohara T 2005 *J. Magn. Magn. Mater.* **288** 339
[16] De K, Majumdar S and Giri S 2007 *J. Appl. Phys.* **101** 103909
[17] De K, Majumdar S and Giri S 2007 *J. Phys. D: Appl. Phys.* **40** 5810
[18] Thakur M, De K, Giri S, Si S, Kotal A and Mandal T K 2006 *J. Phys.: Condens. Matter* **18** 9093
[19] Rivadulla F, Lopez-Quintela M A and Rivas J 2004 *Phys. Rev. Lett.* **93** 167206
[20] Kundu A K, Nordblad P and Rao C N R 2006 *J. Phys.: Condens. Matter* **18** 4809
[21] Pi L, Zhang S, Tan S and Zhang Y 2006 *Appl. Phys. Lett.* **88** 102502
[22] Del Bianco L, Fiorani D, Testa A M, Bonetti E and Signorini L 2004 *Phys. Rev.* B **70** 052401
[23] Meiklejohn W H 1962 *J. Appl. Phys.* **33** 1328